Probing the phase composition of silicon films in situ by etch product detection

Probing the phase composition of silicon films *in situ* by etch product detection

G. Dingemans and M. N. van den Donker[a)]
IEF5-Photovoltaik, Forschungszentrum Jülich GmbH, D-52425 Jülich, Germany and Department of Applied Physics, Eindhoven University of Technology, P.O. Box 513, 5600 MB Eindhoven, The Netherlands

A. Gordijn
IEF5-Photovoltaik, Forschungszentrum Jülich GmbH, D-52425 Jülich, Germany

W. M. M. Kessels[b)] and M. C. M. van de Sanden
Department of Applied Physics, Eindhoven University of Technology, P.O. Box 513, 5600 MB Eindhoven, The Netherlands

(Received 10 August 2007; accepted 25 September 2007; published online 15 October 2007)

Exploiting the higher etch probability for amorphous silicon relative to crystalline silicon, the transiently evolving phase composition of silicon films in the microcrystalline growth regime was probed *in situ* by monitoring the etch product (SiH_4) gas density during a short H_2 plasma treatment step. Etch product detection took place by the easy-to-implement techniques of optical emission spectroscopy and infrared absorption spectroscopy. The phase composition of the films was probed as a function of the SiH_4 concentration during deposition and as a function of the film thickness. The *in situ* results were corroborated by Raman spectroscopy and solar cell analysis. © *2007 American Institute of Physics*. [DOI: 10.1063/1.2799738]

The phase composition of microcrystalline silicon defines its material properties and relates directly to device performance of silicon films in photovoltaic applications.[1] The phase transition from microcrystalline to amorphous silicon draws special attention: optimal performance of amorphous-silicon (*a*-Si:H) films is obtained close to the onset of crystallite nucleation, in the so-called protocrystalline growth regime,[2] whereas best microcrystalline-silicon (μc-Si:H) solar cell absorber layers are generally deposited within a narrow process parameter window just before entering the *a*-Si:H growth regime.[3,4]

In situ spectroscopic ellipsometry has been employed successfully for monitoring the film phase composition during growth,[2] but its implementation imposes constraints on reactor design. Optical emission spectroscopy (OES) is an easy-to-implement *in situ* diagnostic which is applied frequently to monitor process drifts and to relate the relative abundance of emissive species in the deposition process to resulting film properties.[5–10] Due to the importance of the atomic hydrogen to SiH_x radical flux ratio, emission intensity ratios between excited H^* and SiH^* (or Si^*) emission have been correlated to the film crystallinity.[7–10] Nonetheless, such ratios are strictly empirical, reactor dependent, and require *ex situ* calibration.

In this letter we present an approach to probe the μc-Si:H to *a*-Si:H phase transition *in situ* with high accuracy by detecting etch products from the silicon films. Briefly, the method is based on a short H_2 plasma treatment step during which the gas phase density of SiH_4 (i.e., the main etch product released from the film surface) is detected. Atomic hydrogen preferentially inserts into strained Si–Si bonds[11,12] resulting in a higher etch rate of *a*-Si:H relative to μc-Si:H.[13,14] The SiH_4 density in the plasma is observed directly by infrared absorption spectroscopy[15] or, alternatively, indirectly by OES. In the latter method, the SiH^* emission is detected as originating from SiH_4 etch product dissociation by electron impact, as also reported by Westlake and Heintze.[13] We will demonstrate that the SiH^* emission and the SiH_4 density during H_2 plasma treatment correlate with the *a*-Si:H fraction of the as-deposited silicon film.

The experiments were carried out on two capacitively coupled parallel plate reactors equipped with showerhead electrode configuration and driven at 13.56 MHz. In the first reactor the plasma is sustained between two 150 cm^2 electrodes with interelectrode distance of 1.0 cm. Deposition was carried out in the high pressure depletion regime optimized for state-of-the-art solar cells, including a pressure of 10 Torr, a plasma power density of 0.5 W/cm^2, and a substrate temperature of 196 ± 12 °C.[16] The H_2 flow was held constant at 360 SCCM (SCCM denotes cubic centimeter per minute at STP), whereas the SiH_4 flow was used as the main deposition variable ranging from 0 to 8 SCCM. The second reactor is a large area reactor (30×30 cm^2) equipped with infrared spectroscopy in the gas exhaust line. This reactor was used to corroborate the results obtained in the first reactor. The deposition parameters include a pressure of 8 Torr, a power density of 0.4 W/cm^2, and a substrate temperature of 150 °C. The H_2 flow was 2000 SCCM and the SiH_4 flow was varied between 30 and 70 SCCM. In-house prepared ZnO coated Corning glass substrates were used in all experiments. Optical emission spectroscopy measurements were performed through a viewport at the side of the reactor using a high resolution spectrometer.[16] The crystalline volume fraction (I_c^{RS}) of the films was determined from Raman spectra taken at laser wavelengths of 680 and 413 nm and analyzed by the procedure described by Smit *et al.*[17] Solar cell properties were obtained by AM 1.5 illuminated current-voltage measurements using a class A double source solar simulator.

[a)]Present address: Solland Solar Cells BV, Bohr 10, 6422 RL Heerlen, The Netherlands.
[b)]Author to whom correspondence should be addressed. Electronic mail: w.m.m.kessels@tue.nl

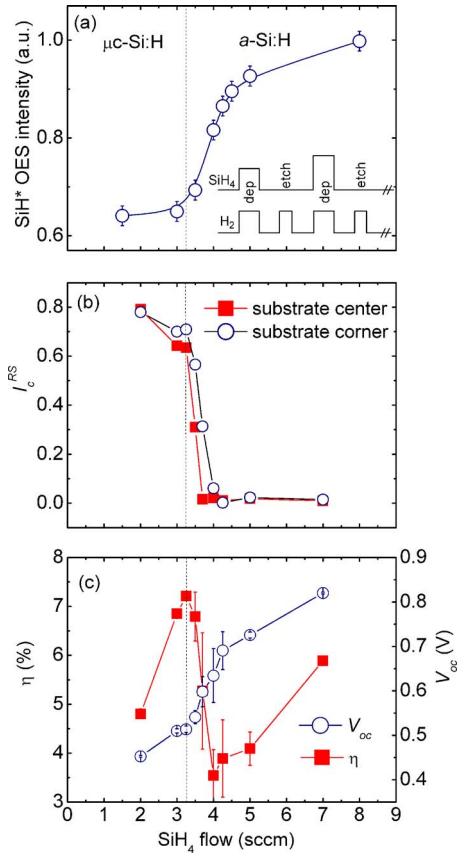

FIG. 1. (Color online) (a) SiH^* emission intensity as obtained by H_2 plasma etching of silicon films deposited under various SiH_4 flows. The inset is a schematic of the experimental procedure employed. (b) Raman crystallinity I_c^{RS} of the silicon films as measured in the center and corner of the substrate. The laser wavelength was 680 nm yielding a Raman penetration depth exceeding the film thickness. (c) Solar energy conversion efficiency η and open circuit voltage V_{oc} for the corresponding thin film silicon *p-i-n* solar cells. No ZnO back reflector was applied.

The experimental procedure to map the phase transition as a function of SiH_4 concentration in the plasma was based on cycles of subsequent deposition and H_2 plasma treatment steps. In every cycle, first an ~150 nm thick silicon film was deposited by the H_2-SiH_4 plasma. Subsequently, after a pump down to <0.1 Torr, a H_2 plasma treatment of the silicon film was carried out using the same H_2 flow, pressure, plasma power, and substrate temperature as applied under deposition (note that these conditions were kept constant within a deposition series). The H_2 plasma treatment time was set at <60 s to diminish H-induced material modification[11,14,18] and the influence of redeposition.[19,20] The time averaged baseline corrected SiH^* emission at 414.3 nm proved to scale with the SiH_4 density[13,21] and is used here as a measure for the abundance of etch products during H_2 plasma treatment. After H_2 treatment the next cycle commences with the deposition of a fresh silicon film on top of the previous film using a different SiH_4 flow. The procedure is schematically represented in the inset of Fig. 1(a).

Figure 1(a) shows the SiH^* emission intensity recorded during H_2 plasma treatment as a function of SiH_4 flow used during deposition of the films. The OES signal is observed to increase rapidly for films deposited at SiH_4 flows above 3.25 SCCM. This increase coincides with a drop in the crystalline volume fraction [Fig. 1(b)] of a *p-i-n* solar cell series in which the silicon films were incorporated as intrinsic absorber layer. The transition toward *a*-Si:H growth as a function of SiH_4 flow starts in the center of the 10×10 cm^2 substrate. This lateral nonuniformity in the transition region, which we tentatively attribute to a nonuniform SiH_x to H flux ratio toward the substrate, is also reflected by the error bars in the solar cell parameters shown in Fig. 1(c). These error bars represent the mean deviation of electronic properties of 18 individual solar cells distributed over the substrate. The open circuit voltage (V_{oc}) is observed to increase from 400–500 mV (typical range for μc-Si:H) to 700–800 mV (typical range for *a*-Si:H).[3,4] The solar energy conversion efficiency (η) is maximal at the point where the OES signal starts increasing, whereas η decreases rapidly in the transition region to *a*-Si:H. The short-circuit current density and fill factor (not shown) show a similar trend as η.

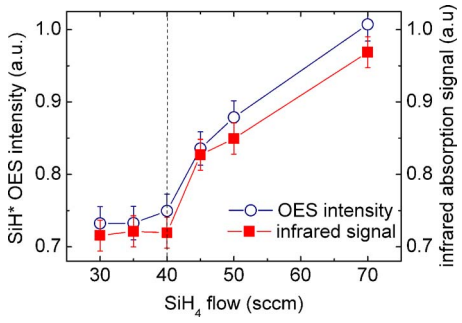

FIG. 2. (Color online) Normalized SiH^* emission intensity and SiH_4 infrared absorption signal at 2189 cm^{-1} during H_2 plasma treatment of silicon films deposited in the large area reactor.

In Fig. 2 the results obtained at the large-area reactor during H_2 plasma treatment of the silicon films are presented. The figure shows the correlation between the SiH^* emission intensity and the SiH_4 infrared absorption signal at 2189 cm^{-1} (Q branch), validating that the SiH^* emission is a measure for the etch product density. The increase of the etch product density in the μc-Si:H to *a*-Si:H transition region indicates an increase in the *a*-Si:H fraction of the silicon films for SiH_4 flows >40±2 SCCM.

From the results on both reactors, it can be concluded that the onset of the μc-Si:H to *a*-Si:H phase transition can be determined accurately even by the easy-to-implement technique of OES. The *in situ* method was also successfully cross checked on various other reactors operating in a wide range of process settings, including a reactor with very-high-frequency plasma excitation and a roll-to-roll deposition reactor. From the results on the different reactors it follows also that the interpretation of the etch product density in terms of the phase composition of the film on the substrate is not significantly complicated by the contribution from etching other reactor surfaces, e.g., the powered electrode.

The robustness of the technique was also demonstrated by its application for depth profiling of the phase composition of films grown under μc-Si:H growth conditions. In these experiments, the phase composition was measured as a function of silicon film thickness using an *a*-Si:H seed layer as starting surface. The deposition-etch cycle consisted out of three steps: (i) the deposition of the *a*-Si:H seed layer to create a well-defined amorphous starting surface, (ii) the deposition of a silicon film under μc-Si:H growth conditions (2 SCCM SiH_4 and 360 SCCM H_2), and (iii) a short H_2 plasma treatment to probe the crystallinity of the silicon film in the surface region. The thickness of the silicon film depos-

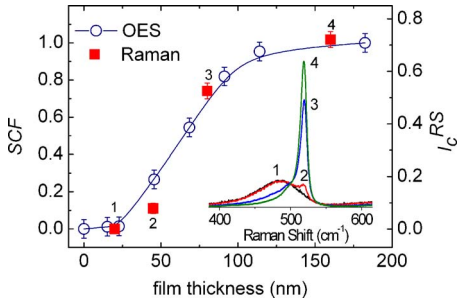

FIG. 3. (Color online) The surface crystallinity fraction SCF determined by etch product detection by OES as a function of the silicon film thickness deposited under μc-Si:H growth conditions on top of an *a*-Si:H seed layer. The data are compared to the Raman crystallinity I_c^{RS} measured at a laser wavelength of 413 nm for selected samples. The corresponding Raman spectra are shown as inset.

ited in step (ii) was varied per cycle to obtain the change in crystallinity as a function of film thickness. The SiH^* emission during H_2 plasma treatment was linearly converted to a so-called surface crystallinity fraction (SCF) as the crystallinity of the films in the surface region was probed. SCF is defined equal to unity for steady state μc-Si:H growth conditions [corresponding to the lower plateau in Figs. 1(a) and 2] and equal to 0 for the *a*-Si:H seed layer. The crystalline volume fraction of the silicon films in the surface region was also measured using Raman spectroscopy with a 413 nm laser with a reduced film penetration depth ($<$20–30 nm). This measurement was carried out on selected films covering the thickness range of interest. The results for both the SCF and the Raman crystallinity as a function of the thickness of the film deposited under μc-Si:H growth conditions are shown in Fig. 3. The surface crystallinity remains relatively constant for small film thicknesses (up to 25 ± 10 nm), indicating predominantly *a*-Si:H surface properties. Subsequently the SCF increases with film thickness (i.e., the OES signal and H_2 plasma induced etch rate decreased) representing the onset of a mixed-phase regime consisting of both crystalline and amorphous materials. Finally, at a thickness of 125 ± 25 nm, the SCF starts to saturate when single-phase microcrystalline silicon is formed and steady state growth is reached. The Raman crystallinity data I_c^{RS} show good agreement with the SCF values obtained by the OES method. The general features of the μc-Si:H growth process in Fig. 3 as deduced from *in situ* etch product monitoring measurements are consistent with reports in the literature.[2,3,22] Starting on an amorphous seed layer, deposition evolves from an initial *a*-Si:H incubation phase, through a mixed-phase region with both microcrystalline and amorphous materials, toward single-phase μc-Si:H. Additional experiments employing etch product monitoring revealed that the thicknesses of the incubation- and the mixed-phase regions are critically depending on the SiH_4 concentration in the H_2-SiH_4 plasma.

In conclusion, we demonstrated that the difference in etch rate between μc-Si:H and *a*-Si:H by atomic hydrogen can be exploited to determine the phase composition of silicon films *in situ* by etch product detection. The validity of the technique, employing both optical emission spectroscopy and infrared spectroscopy, was cross checked at various reactor configurations and the technique was successfully applied to probe the *a*-Si:H to μc-Si:H transition as a function of process conditions and film thickness. Etch product monitoring facilitates therefore a fast, noninvasive, and accurate exploration of deposition regimes with optimized process conditions as well as the investigation of μc-Si:H incubation effects. Consequently, the technique is expected to contribute to technological developments toward silicon film deposition regimes yielding high solar energy conversion efficiencies under improved economically viable conditions.

The authors thank K. Nadir (TU Eindhoven), R. Schmitz, J. Kirchhoff, M. Hülsbeck, and W. Appenzeller (Forschungszentrum Jülich) for technical assistance and Dr. R. Carius, Dr. D. Hrunski (Forschungszentrum Jülich), Dr. B. Rech (Hahn-Meitner Institute), and Dr. E. Hamers (Helianthos) for fruitful discussions.

[1] A. Shah, P. Torres, R. Tscharner, N. Wyrsch, and H. Keppner, Science **285**, 692 (1999).
[2] R. W. Collins, A. S. Ferlauto, G. M. Ferreira, C. Chen, J. Koh, R. J. Koval, Y. Lee, J. M. Pearce, and C. R. Wronski, Sol. Energy Mater. Sol. Cells **78**, 143 (2003).
[3] O. Vetterl, F. Finger, R. Carius, P. Hapke, L. Houben, O. Kluth, A. Lambertz, A. Mück, B. Rech, and H. Wagner, Sol. Energy Mater. Sol. Cells **62**, 97 (2000).
[4] S. Klein, F. Finger, R. Carius, and M. Stutzmann, J. Appl. Phys. **98**, 024905 (2005).
[5] M. N. van den Donker, B. Rech, F. Finger, W. M. M. Kessels, and M. C. M. van de Sanden, Appl. Phys. Lett. **87**, 263503 (2005).
[6] M. N. van den Donker, S. Klein, B. Rech, F. Finger, W. M. M. Kessels, and M. C. M. van de Sanden, Appl. Phys. Lett. **90**, 183504 (2007).
[7] J. K. Rath, R. H. J. Franken, A. Gordijn, R. E. I. Schropp, and W. J. Goedheer, J. Non-Cryst. Solids **338-340**, 56 (2004).
[8] L. Guo, M. Kondo, M. Fukawa, K. Saitoh, and A. Matsuda, Jpn. J. Appl. Phys., Part 1 **37**, 1116 (1998).
[9] Y. Fukuda, Y. Sakuma, C. Fukai, Y. Fujimura, K. Azuma, and H. Shirai, Thin Solid Films **386**, 256 (2001).
[10] L. Feitknecht, J. Meier, P. Torres, J. Zürcher, and A. Shah, Sol. Energy Mater. Sol. Cells **74**, 539 (2002).
[11] S. Sriraman, S. Agarwal, E. S. Aydil, and D. Maroudas, Nature (London) **418**, 62 (2002).
[12] J. J. Boland and G. N. Parsons, Science **256**, 1304 (1992).
[13] W. Westlake and M. Heintze, J. Appl. Phys. **77**, 879 (1995).
[14] O. Vetterl, P. Hapke, L. Houben, F. Finger, R. Carius, and H. Wagner, J. Appl. Phys. **85**, 2991 (1999).
[15] B. Strahm, A. A. Howling, L. Sansonnens, and Ch. Hollenstein, Plasma Sources Sci. Technol. **16**, 80 (2007).
[16] M. N. van den Donker, R. Schmitz, W. Appenzeller, B. Rech, W. M. M. Kessels, and M. C. M. van de Sanden, Thin Solid Films **511-512**, 562 (2006).
[17] C. Smit, R. A. C. M. M. van Swaaij, H. Donker, A. M. H. N. Petit, W. M. M. Kessels, and M. C. M. van de Sanden, J. Appl. Phys. **94**, 3582 (2003).
[18] I. Kaiser, N. H. Nickel, W. Fuhs, and W. Pilz, Phys. Rev. B **82**, 1718 (1998).
[19] K. Saitoh, M. Kondo, M. Fukawa, T. Nishimiya, A. Matsuda, W. Futako, and I. Shimizu, Appl. Phys. Lett. **71**, 3403 (1997).
[20] S. Veprek and V. Marecek, Solid-State Electron. **11**, 683 (1968).
[21] M. N. van den Donker, B. Rech, W. M. M. Kessels, and M. C. M. van de Sanden, New J. Phys. **9**, 280 (2007).
[22] M. Tzolov, F. Finger, R. Carius, and P. Hapke, J. Appl. Phys. **81**, 7376 (1997).